

Exocytotic fusion pore stability and topological defects in the membrane with orientational degree of ordering

Dalija Jesenek^a, Šárka Perutková^b, Veronika Kralj-Iglič^{c,d}, Samo Kralj^{a,e}, Aleš Iglič^{b,d,*}

^a Department of Condensed Matter Physics, J. Stefan Institute, SI-1000 Ljubljana, Slovenia

^b Laboratory of Biophysics, Faculty of Electrical Engineering, University of Ljubljana, Tržaška cesta 25, SI-1000 Ljubljana, Slovenia

^c Faculty of Health Studies, University of Ljubljana, Zdravstvena 5, SI-1000 Ljubljana, Slovenia

^d Laboratory of Clinical Biophysics, Department of Orthopaedics, University of Ljubljana, Zaloška 9, SI-1000 Ljubljana, Slovenia

^e Department of Physics, Faculty of Natural Sciences and Mathematics, University of Maribor, SI-2000 Maribor, Slovenia

ARTICLE INFO

Article history:

Received 5 March 2012

Received in revised form 26 March 2012

Accepted 2 April 2012

Available online 26 April 2012

Keywords:

Regulated exocytosis

Fusion pore

Orientational ordering of membrane

components

Topologically driven defects

ABSTRACT

Regulated exocytosis is a process that strongly depends on the formation and stability of the fusion pore. It was indicated experimentally and theoretically that narrow and highly curved fusion pore may be stabilized by accumulation of anisotropic membrane components possessing orientational ordering. On the other hand, narrow fusion pore may also undergo repetitive opening and closing, disruption in the so called kiss and run process or become completely opened in the process of full fusion of the vesicle with the membrane. In this paper we attempt to elucidate the subtle interplay between the stabilizing and destabilizing processes in the fusion neck. A possible physical mechanism which may lead to disruption of the stable fusion pore or complete fusion of the vesicle with the membrane is discussed. It is indicated that topologically driven defects of the in-plane orientational membrane ordering in the region of the fusion pore may disrupt the fusion. Alternatively, it may facilitate repetitive opening and closing of the fusion pore or induce full fusion of the vesicle with the target membrane.

© 2012 Elsevier Ltd. All rights reserved.

1. Introduction

Membrane shape changes are linked to several cellular processes of vital biological importance such as endocytosis and exocytosis [1–5] and may be provoked by varying external conditions such as temperature, binding/adhering of nanoparticles (proteins, colloids) or by formation of topological defects in nematic orientational order within a biological membrane. In this paper, possible changes in exocytosis process driven by topological defects in nematic orientational ordering of membrane constituents are considered.

Membrane surface might exhibit a tangential (in-plane) orientational ordering [6]. For example, such ordering may arise due to the in-plane (averaged) orientational ordering of lipid molecules due to their intrinsic anisotropic shape [7–9] or due to tilting of lipid molecules relative to the normal of the membrane [11]. Besides the lipids, also dimeric amphiphiles [10] and the membrane embedded anisotropic proteins or the membrane-attached proteins (like for

example I-BAR or rod-like F-BAR domain containing proteins) may undergo orientational ordering within the membrane [12–17].

One of the first studies of the impact of the in-plane ordering on membrane shape was performed by MacKintosh and Lubensky [18] using a mean-field theory. These and some other studies [7,17,19] indicated that the coupling between in-plane ordering of membrane anisotropic components and membrane mechanical properties could trigger transitions between spherical and cylindrical shapes of vesicles or vesicle protrusions. It was shown experimentally that strongly anisotropic dimeric amphiphiles induce tubular membrane budding while isotropic amphiphiles promote spherical membrane budding [10]. Also it was shown [11,20] that in-plane ordering might suppress vesicle structures exhibiting neck-type profiles. On the other hand it was indicated that in-plane ordering of saddle-like membrane components may stabilize highly curved membrane necks [4,8,14].

Membrane fusion is an essential event in many biological processes of eukaryotic cells [1–3,21]. It is assumed to begin with the formation of an intermediate structure (hemi-fusion stalk) connecting the outer leaflets of fusing membranes (for review see Refs. [22,23]). Hemi-fusion stalk then proceeds into a fusion neck (pore), the membrane bilayer channel connecting a spherical vesicle and plasma membrane [4] (Fig. 1). After formation, the fusion neck may either close so the vesicle can be involved in another round of exocytosis [4,24], or it fully opens [5], leading to full fusion exocytosis,

* Corresponding author at: Laboratory of Biophysics, Faculty of Electrical Engineering, University of Ljubljana, Tržaška cesta 25, SI-1000 Ljubljana, Slovenia. Tel.: +386 1 4768 825; fax: +386 1 4768 850.

E-mail address: ales.iglic@fe.uni-lj.si (A. Iglič).

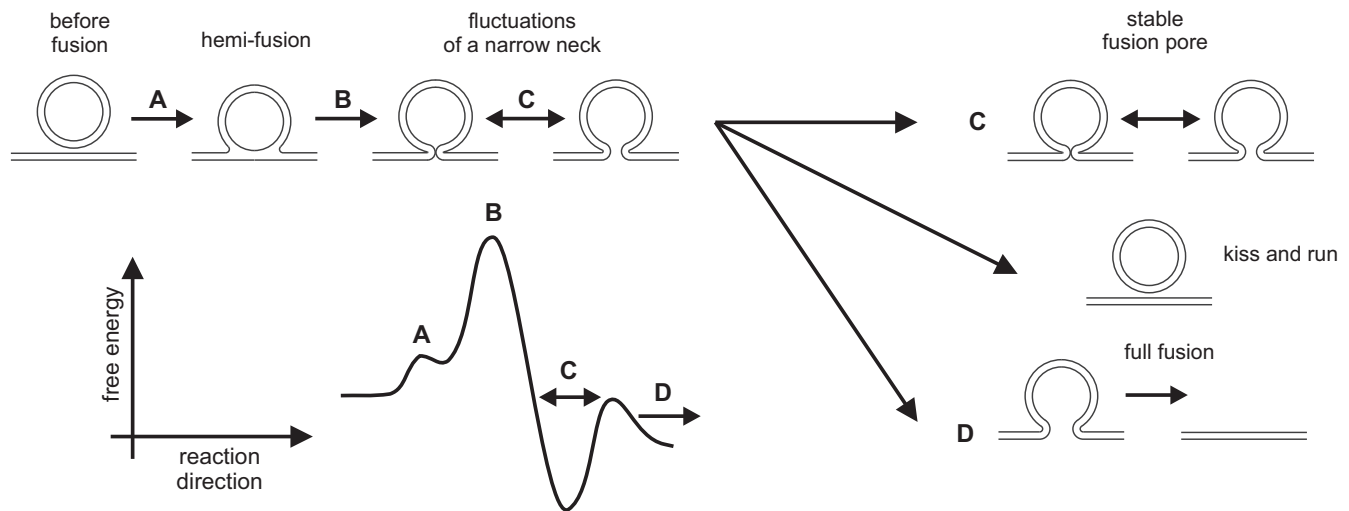


Fig. 1. Fusion of vesicle and the plasma membrane is believed to begin with the formation of a hemi-fusion stalk (transition A), an intermediate structure connecting the outer leaflets of fusing membranes (for review see [23]). Hemi-fusion stalk then develops into a fusion pore (transition B) which may become stable [4] and can therefore reversibly vary its diameter around its “equilibrium” value (transitions C). Vesicles in state C may transit into a state with wider fusion neck diameter and further into a state of full fusion. The fusion pore can be also disrupted (kiss and run scenario) [5] or it remains stable for longer time in state C [4].

i.e. complete merge of the vesicle membrane with the target cell plasma membrane [4,25]. The fusion pore can be also disrupted, so the vesicle is detached from the plasma membrane (kiss and run scenario) [5] (Fig. 1). It is also possible that the fusion pore remains stable. In this case the membrane fused vesicle serves as a docking site for other exocytic membranes (secondary fusion events) generating a chain of interconnected vesicles [5].

At the first glance a formation of the fusion pore may be considered as energetically unfavorable due to repulsive electrostatic forces between the two closely apposed phospholipid bilayers. These forces need to be overcome in order to reach the metastable transition states (Fig. 1) leading to the fusion neck formation [26]. However, the repulsive electrostatic forces can be reduced or even transformed to attractive forces, for example by the charged nanoparticles mediated interactions [27–29]. Another example of the possible mediators is SNARE (soluble N-ethylmaleimide-sensitive factor attachment protein receptor [30]).

It was suggested that without stabilizing factors the fusion pore would spontaneously close or open in a short time period [31]. On the other hand some recent experimental results [4,32,33] indicated the possibility of formation of a stable thin membrane neck connecting the vesicle and plasma membrane [4]. In addition to some proteins, also negatively charged lipid molecules have been shown to strongly affect the probability of exocytosis [35].

Recently the experimentally observed stability of fusion pore was explained [4] within the theoretical model of multicomponent bilayer membrane. It was shown that due to high (anisotropic) curvature in the region of the fusion neck a strong lateral and orientational redistribution of anisotropic membrane constituents in this thin membrane region may contribute to a strong decrease of the membrane free energy (i.e. energy minimum C in Fig. 1) [4,14] which may stabilize the fusion pore. Namely, in the fusion pore the difference between the two principal membrane curvatures is very high, reaching the regime where the anisotropic intrinsic shape of the membrane constituents becomes locally and globally important because of average membrane in-plane orientational ordering of anisotropic membrane constituents [4,8,9,12,14,19,34].

The equilibrium fusion pore diameter stabilized by local accumulation of isotropic inverted conical inclusions is much wider (i.e. more than 50 nm wide) than the pore stabilized by accumulation of anisotropic membrane components and does not correspond to

the experimentally determined values of the order of magnitude of 1 nm given in [4].

Although exocytotic fusion pore was hitherto believed to be energetically unfavorable in the absence of specific stabilizing factors [36], repetitive fusion pore events in resting lactotrophs [4,32,33] indicate (in agreement with theoretical predictions [4]) that thin fusion pore may be energetically favorable and likely entrapped in an energy minimum of state C as shown in Fig. 1 [4].

However, as schematically shown in Fig. 1 the fusion neck can be also disrupted (kiss and run scenario) or fully opened, leading to complete merge of the vesicle membrane with the target plasma membrane [5]. This would not be possible if in addition to the pore stabilization factors (reflected in the local minimum C of the free energy as presented in Fig. 1) there would not exist some additional physical mechanism leading to disruption of the neck (kiss and run scenario) or favoring the complete fusion of the vesicle, i.e. the jump across the energy barrier from the state C to state D as shown in Fig. 1.

Therefore we next theoretically discuss the nature of the possible physical mechanism which may lead to disruption of the stable fusion pore or alternatively the complete fusion of the vesicle where the fusion pore is assumed to be stabilized by the local accumulation and orientational ordering of anisotropic membrane constituents. We attempt to uncover the subtle interplay between the stabilizing and destabilizing physical processes in the fusion pore based on the very general physical principles. Our main assumption is that topologically driven defects [37,38] in the membrane with orientational degree of ordering may contribute to disruption of the fusion pore or alternatively facilitate the transition to a full fusion of vesicle (Fig. 1). To ascertain the plausibility of our model we shall present the corresponding theoretical analysis taking into account the membrane in-plane orientational degree of freedom. In our present model the ordering is described by using a tensor order parameter which allows us to analyze also cores of topological defects.

2. Theoretical background

2.1. Topology and topological defects

In the case of in-plane membrane orientational ordering topological defects unavoidably appear due to topological reasons [37].

The total sum of topological charges m_{tot} of all defects residing on a membrane surface is determined by a theorem of Poincaré [39]. It claims that m_{tot} must equal the Euler–Poincaré characteristic $\chi = 2(1 - g)$ of the surface. The integer g is the genus of the surface, reflecting to the number of “handles” that the surface contains. For example, an object exhibiting spherical topology is characterized by $g=0$ and consequently $m_{tot}=2$ [40]. The topological number χ is determined by the total Gaussian curvature K of the surface. In addition, spatial dependence of K could have strong impacts on position and also number of defects. Vitelli and Turner [41] showed that positive (negative) K attracts defects with positive (negative) topological charge m . Furthermore, interactions among defects resemble interaction among electrical charges. Namely, defects with a same sign of m in general repel each other while defects of opposite topological charge exhibit attraction. Furthermore, surfaces possessing both negative and positive Gaussian curvature might trigger unbinding of topological pairs defect–antidefect.

In the paper we study the space distribution of topological defects in axial-symmetric shapes involving fusion pore which is important to simulate the process of exocytosis. The minimal model is used allowing to study curvature driven formation of additional topological defects.

2.2. Model

A membrane possessing in-plane orientational ordering is considered. A simplest possible model is used where the membrane is treated as a two dimensional object embedded in the three dimensional Euclidean space. The local orientational order is described in terms of the traceless and symmetric tensorial order parameter [38,42]

$$\mathbf{Q} = \lambda(\bar{n} \otimes \bar{n} - \bar{n}_\perp \otimes \bar{n}_\perp). \quad (1)$$

Here \bar{n} and \bar{n}_\perp are normalized eigenvectors of \mathbf{Q} . The corresponding eigenvalues are $\lambda \in [0, 1/2]$ and $-\lambda$, respectively. The orientational field \bar{n} points along an average in-plane local orientation. The head-to-tail invariance is imposed, therefore $\pm\bar{n}$ states are physically equivalent. The maximal degree of orientational order corresponds to $\lambda = 1/2$. On the other hand the orientational order vanishes (i.e., it is melted) when $\lambda = 0$.

A local membrane normal is determined by $\bar{v} = \bar{n} \times \bar{n}_\perp$ and its shape is determined by a curvature tensor \mathbf{C} . Its eigenvalues C_1 and C_2 are the principal curvatures along orthogonal directions within the membrane. The local mean curvature H and the Gaussian curvature K can be expressed as $H = (1/2)\text{Tr}\mathbf{C} = (1/2)(C_1 + C_2)$ and $K = \text{Det}\mathbf{C} = C_1 C_2$, where Tr and Det stand for the trace and determinant operation, respectively. We also introduce curvature deviator $D = \sqrt{(H^2 - K)}$. We further assume that membranes intrinsic local ordering is imposed by intrinsic mean curvature H_m and intrinsic curvature deviator D_m .

The orientational free energy term per unit area f_{ord} [38] determines orientational ordering for a given geometry:

$$f_{ord} = \frac{A_0 t}{2} \text{Tr}\mathbf{Q}^2 + \frac{B}{4} \text{Tr}\mathbf{Q}^4 + \frac{k}{2} |\nabla_s \mathbf{Q}|^2 - \frac{k_{24} K}{2} \text{Tr}\mathbf{Q}^2. \quad (2)$$

Lowest order symmetry allowed terms needed for our description are only considered. Derivation details are described in Ref. [38]. The first two terms determine equilibrium bulk ordering in flat geometry. Quantities A_0 and B are material constants, $t = T - T_c/T_c$ stands for the reduced temperature, and T_c describes the bulk phase transition temperature between orientationally disordered and ordered phase. In bulk equilibrium value of order parameters is equal to $\lambda_b = \sqrt{-tA_0/(2B)}$ for $t < 0$. For $t > 0$ the order is melted.

The remaining terms in Eq. (2) determine orientational elastic free energy penalties, where k and k_{24} are elastic constant and ∇_s marks the surface gradient operator. Note that introduction of a

single constant k assumes that bend and splay-type deformations of \bar{n} are equally weighted. The constant k_{24} is related to the saddle splay elastic constant in description of nematic liquid crystal ordering in three dimensions. Its contribution renormalizes local effective temperature. Competition between the condensation and elastic terms in Eq. (2) defines the order parameter correlation length $\xi \sim \sqrt{k/|A_0 t|}$.

The lowest order symmetry allowed coupling free energy term (per unit area) is given by [43]

$$f_{cp} = k_{cp} \text{Tr}(\mathbf{Q}\mathbf{C}), \quad (3)$$

where k_{cp} stands for the coupling constant.

We minimize the free energy $F = \iint f da$ of an axially symmetric membrane, where $f = f_{ord} + f_{cp}$. Here the integral is carried over the total surface of the membrane and da stands for an infinitesimal surface area. In solving equations we adopt a constant volume constraint. Therefore, the membrane shape and orientational ordering are coupled indirectly. Variational parameters of the model are the membrane shape and orientational ordering within the membrane surface.

In our simulation we calculate the degree of orientational ordering of an axially symmetric membrane by minimizing the free energy contribution f_{ord} with respect to \mathbf{Q} for a given membrane shape. We assume that the coupling constant k_{cp} is negligibly small. Furthermore, we assume that the membrane curvature energy dominantly determines the shape of membrane. Namely, the calculated shapes are close to limiting shapes and can be therefore approximately determined by minimization of the membrane curvature energy only [8] as described in detail in [4].

3. Results

We focus on orientational ordering defects in process of membrane fusion schematically shown in Fig. 1. We assume that the condition for the in-plane orientational order is fulfilled. In the following we demonstrate typical ordering textures before and after the fusion. In the latter case we consider only the (transient) stable fusion pore stage shown in Fig. 1.

3.1. Pre-fusion regime

For illustration purpose we set that prior to fusion both objects have roughly spherical symmetry. Small deviations from this shape would only result in slightly different relative position of topological defects. Furthermore, we set that the radii characterizing both elements are large with respect to order parameter correlation length ξ . Consequently, orientational order is globally established except at defect sites. Typical degree of ordering in each element of the system prior to merging is shown in Fig. 2. The spherical topology enforces topological defects with the total topological charge $m_{tot} = 2$. For conditions described in Fig. 2 four topological defects with topological charge $m = 1/2$ are formed. Because the Gaussian curvature is spatially homogeneous the repulsing interaction among defects dominantly influences their relative position. In this case four defects with topological charge $m = 1/2$ occupy vertices of a tetrahedron in order to maximize their mutual separation. In Fig. 2a the degree of ordering λ is superimposed on the membrane structure. At defect sites the orientational field is not uniquely defined and corresponding high elastic penalties give rise to local melting. Therefore, exact positions of defects are signaled by local points where $\lambda = 0$. This is clearly shown in Fig. 2b where we plot spatial evolution in the planar membrane coordinate system (ψ, ϑ) . Here the coordinates $\psi \in [0, 2\pi]$ and $\vartheta \in [0, \pi]$ determine meridians and parallels of the spherical membrane. Note that defect textures of both spheres differ only in the size of defect cores

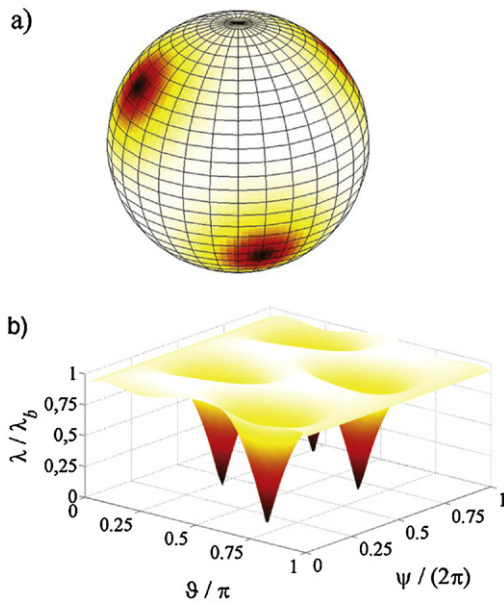


Fig. 2. (a) Degree of orientational ordering λ superimposed on a spherical membrane. The membrane hosts 4 topological defects with $m = 1/2$. The total topological charge is therefore $m_{tot} = 2$. (b) Degree of orientational order in the (ψ, ϑ) plane where the angles ψ and ϑ stand for the azimuthal and zenithal angle, respectively. Therefore, parallels are determined by constant value of ϑ and meridians by a constant value of ψ . The bulk degree of orientational order is determined by λ_b . $R/\xi = 8.6$, where R is the radius of the structure and ξ the order parameter correlation length.

(their linear size is roughly given by ξ), within which the degree of ordering is essentially melted.

3.2. Transient stable fusion pore

We next consider typical scenarios which are expected in the *transient stable fusion pore* stage. A typical profile is shown in Fig. 3. For illustration purpose we separately depict ordering in the *outer* and *inner part* of the system, as defined in Fig. 3. Typical geometries of both parts are shown at the right part of the figure. Their typical linear size is determined by R_o (the outer part) and R_i (the inner part). The necks of structures enforce a negative Gaussian curvature which is known to attract topological defects with negative

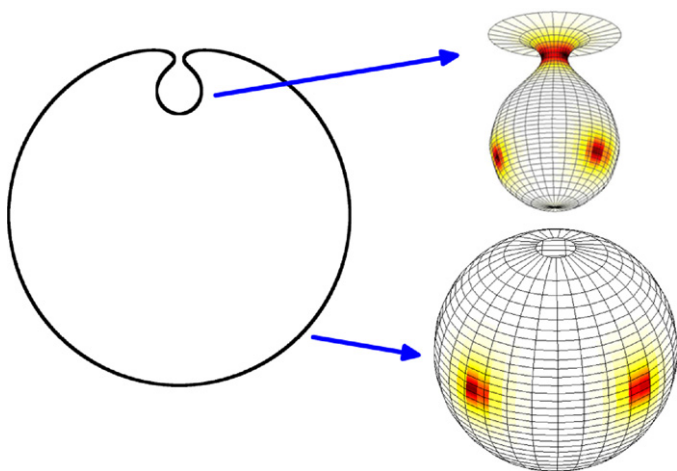


Fig. 3. Schematic presentation of the (transient) *stable fusion pore* structure. It consists of the *inner* and *outer part*. The *outer part* (the bottom structure at the right side) is roughly spherical and therefore exhibits everywhere positive Gaussian curvature. On the contrary, the *inner part* (the top structure at the right side) possesses regions with positive and negative (the neck region) value of K .

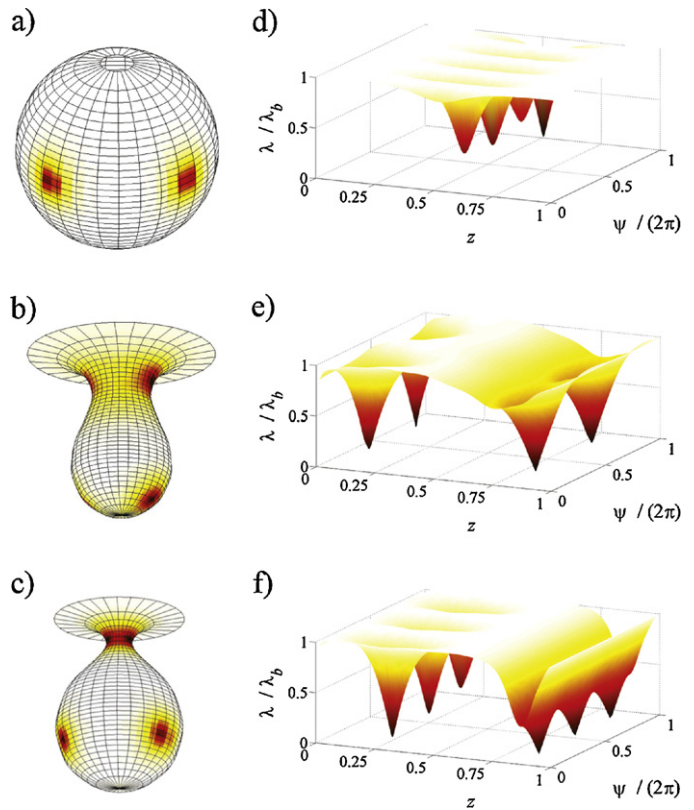


Fig. 4. Defect structure within selected parts of the (*transient*) *stable pore* structure shown in real geometry (a–c) and in the rectangular (ψ, z) plane (d–f). Here ψ stands for the azimuthal angle and z measures distance along the axis of symmetry. Here $z = 0$ and $z = 1$ correspond to the bottom and top part of the structure. The total topological charge of the whole (*transient*) *stable pore* structure equals $m_{tot} = 2$. Note that the total topological part in the *inner* and *outer part* is always 0 and 2, respectively. (a and d) The *outer part*. A possible configuration hosting 4 defects with $m = 1/2$. (b and e) The *inner part*. If the curvature at the neck is strong enough unbinding of defect pairs is realized. In the case shown two antidefects ($m = -1/2$) are localized at the neck where $K < 0$ and the corresponding partner-defects ($m = 1/2$) are assembled in the region where $K > 0$. (c and f) The *inner part*. For even stronger curvature in comparison to (b and e) at the neck additional pair of defects forms. In this case the neck hosts 3 antidefects and the accompanying 3 defects of the *inner part* are assembled in the region where $K > 0$. The defects were calculated for (a and d) $R_o/\xi = 8.6$, (b and e) $R_i/\xi = 27.7$ and (c and f) $R_i/\xi = 43.3$. Here R_o and R_i are typical linear sizes of *outer* and *inner part*, respectively, and ξ the order parameter correlation length.

topological charge. For appropriate conditions this might trigger appearance of additional defects via defect–antidefect unbinding process, where defects (antidefects) are characterized with positive (negative) topological charge. Note that the total topological charge of the *transient stable fusion pore* structure equals to $m_{tot} = 2$. Therefore, a relative position of defects compromises interactions among defects and coupling between a defect and a local Gaussian curvature. Defects of equal signs tend to repel and those of different signs tend to attract each other. Furthermore, Gaussian curvature affects topological defects in a similar manner as an electric field influences electrical charges. Namely, positive K attracts defects with $m = 1/2$ while negative K attracts defects with $m = -1/2$.

Common qualitatively different defect configurations expected in *transient stable fusion pore* structures are shown in Fig. 4 where we either show the *inner* or *outer part* of a structure. In Fig. 4a–c, we show defect structure in geometrical space and in Fig. 4d–f in corresponding rectangular parameter space.

If minimal negative Gaussian curvature is not strong enough then structures exhibit 4 defects with $m = 1/2$. Note that an isolated defect tends to go to the *inner part* of a structure, because it exhibits larger positive value of K in comparison with the *outer part*. However, repelling interaction among positive defects favor the *outer*

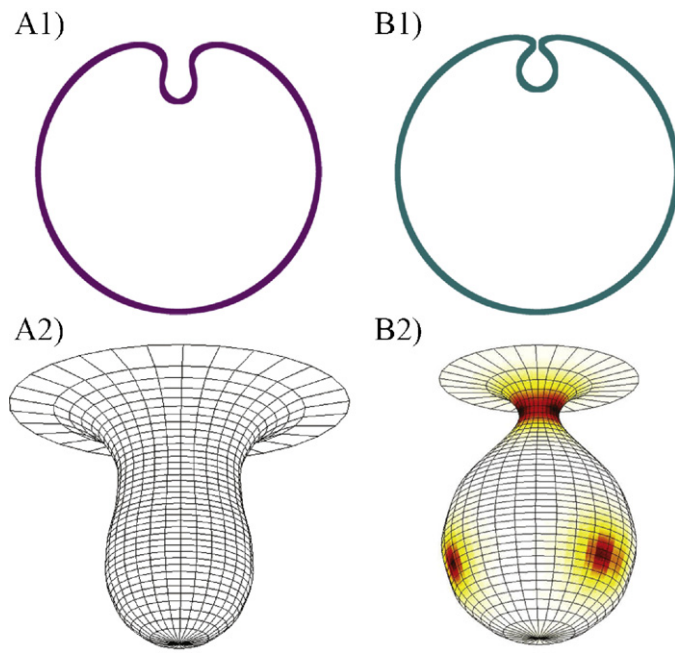


Fig. 5. Schematic presentation of possible different defect structures in the (*transient*) stable pore structure on increasing curvature strength at the neck region (A1 and B1). All structures exhibit topological charge $m_{tot} = 2$. In all cases 4 defects with $m = 1/2$ are confined to the *outer part* of the structure. The defect configurations in the *inner part* structures on increasing the neck-curvature strengths are as follows: (A2) no defects are present, (B2) 3 defects and 3 antidefects are formed.

part of the structure where relative separation of defects could be larger. Our simulations suggest that these four defects always remain in the *outer region*. In addition to structures similar to the one shown in Fig. 2 also other relative positions of defects might be realized. For example, in Fig. 4a and d we illustrate the case where all defects are assembled at the equator.

If curvature at the pore (neck) is not strong enough no additional defects appear. However, for strong enough elastic distortions defect–antidefect pairs might appear. In Fig. 4b and e we show the case where two pairs appear. In addition to 4 defects, which existed prior to the unbinding process, 4 additional defects are formed in the *inner part*. The two newly created positive defects are assembled in the region exhibiting $K > 0$ and corresponding defects with $m = -1/2$ at the neck where $K < 0$. Therefore, the whole structure possesses now 8 defects (6 with $m = 1/2$ and 2 with $m = -1/2$) where the total charge $m_{tot} = 2$ is conserved.

For even stronger elastic distortions at the neck 3 defects pairs are formed which is depicted in Fig. 4c and f. In this case 6 defects appear in the *inner part* of the structure. Defects with $m = 1/2$ are assembled in the region $K > 0$ and defects with $m = -1/2$ at the neck.

In Fig. 5 we schematically plot the dependence of the defects distribution in the fusion vesicle on the increasing curvature (i.e. decreasing diameter) of the pore region. Figures illustrate that on increasing the curvature strength additional pairs of defects appear in the inner part of the structure. Note that antidefects are always localized at the neck.

4. Conclusions and discussion

The observed repetitive transient fusion events were explained by stabilizing effect of accumulation of anisotropic membrane components with in-plane ordering in the region of the fusion pore [4]. The repetitive fusion events are assumed to represent interactions of the same vesicle with the plasma membrane [4,32,33], i.e. repetitive opening and closing of the stable fusion pore (state

C in Fig. 1). Stabilizing in-plane ordering of anisotropic membrane components was shown to strengthen with decreasing radius of the fusion pore. The corresponding membrane free energy is at the same time decreased (at small enough fusion pore radius) [4] pushing the system in direction to the local minimum in the membrane free energy corresponding to the transient equilibrium state (state C in Fig. 1) of the fusion pore. The experimentally observed increase of the fusion pore stability with decreasing fusion pore radius agrees well with this theoretical prediction [4]. However, the repetitive (periodic) transient opening and closing of the stable fusion pore (state C in Fig. 1) were observed also in the absence of stimulation [4,32,33]. In addition, the transient stable fusion pore may be also disrupted (kiss and run scenario) or completely opened in the process of full fusion (Fig. 1). The physical nature of these phenomena is still poorly understood. To answer the question what drives periodic opening and closing of the transient stable fusion pore in state C, its complete opening or even its disruption in the kiss and run process (see Fig. 1), an additional and complementary physical (destabilizing) mechanism governing the dynamics of the fusion pore at small pore radii is suggested in this work.

The suggested opposing destabilizing mechanism is based on the formation of the topological defects which appear in the fusion pore at small enough pore radius (see Fig. 5). Due to (anti)defects in orientational ordering in the region of the fusion pore (see panels B1 and B2 in Fig. 5) the depth of the energy minimum C in Fig. 1 is decreased which may lead to complete opening of the fusion pore (full fusion).

On the other hand, at large enough pore radius where the topological antidefects in the membrane region of the fusion pore disappear (see panels A1 and A2 in Fig. 5) the consequent recovery of the local orientational ordering in the fusion pore region may push the membrane in direction of the pore thinning. In accordance with some experimental observations [4,32,33] the fusion pore dynamics can be described as a repetitive opening and closing of the stable fusion pore (i.e. as a repetitive fusion events of the same vesicle with the plasma membrane). However, it is also possible that the appearance of the topological antidefects in the fusion pore membrane at small radii of the fusion pore (as presented in panels B1 and B2 in Fig. 5) and the consequent loss of the local orientational ordering, push the membrane to the region D of the free energy landscape (see Fig. 1), where the “downhill” force favors complete opening of the pore (full fusion) as schematically shown in Fig. 1. The third possibility (i.e. the disruption of the fusion pore due to the loss of the local orientational ordering in the fusion pore as a consequence of topological (anti)defects at small radii of the pore (panel B2 in Fig. 5) leads to the “kiss and run” scenario (see Fig. 1).

Which of the above described three scenarios of the dynamics of the narrow fusion pore is actually taking place depends on the physical properties of the molecules accumulated in the membrane of the fusion pore (i.e. on the local membrane non-homogeneous and anisotropic mechanical properties) and the relative strength of the two opposing mechanisms determining the stability and dynamics of the fusion pore, i.e. stabilizing mechanism due to accumulation of the anisotropic membrane components subjected to strong orientational ordering [4] and the destabilizing mechanism due to local topologically induced antidefect in the orientational ordering. Further theoretical and experimental studies are needed to better characterize the subtle interplay between these two mechanisms determining the stability and dynamics of the fusion neck.

Conflict of interest statement

There is no conflict of interest regarding this work.

Acknowledgement

This work was supported by Slovenian Research Agency (ARRS) grants J3-2120, J1-4109, J1-4136, J3-4108 and P2-0232.

References

- [1] G.Q. Bi, M.J. Alderton, A.R. Steinhardt, Calcium-regulated exocytosis is required for cell membrane resealing, *Journal of Cell Biology* 131 (1995) 1747–1758.
- [2] S.H. Gerber, C. Thomas, Südhof insulin release: some molecular requisites molecular determinants of regulated exocytosis, *Diabetes* 51 (Suppl. 1) (2002) S3–S11.
- [3] Z. Zhang, M.B. Jackson, Membrane bending energy and fusion pore kinetics in Ca^{2+} -triggered exocytosis, *Biophysical Journal* 98 (2010) 2524–2534.
- [4] J. Jorgačevski, M. Fošnarič, N. Vardjan, et al., Fusion pore stability of peptidergic vesicles, *Molecular Membrane Biology* 27 (2010) 65–80.
- [5] A. Masedunskas, N. Porat-Shliom, R. Weigert, Regulated exocytosis: novel insights from intravital microscopy, *Traffic* (2012) 0854–1600.
- [6] W. Helfrich, J. Prost, Intrinsic bending force in anisotropic membranes made of chiral molecules, *Physical Review A* 38 (1988) 3065–3068.
- [7] V. Kralj-Iglič, A. Iglič, G. Gomišček, F. Sevšek, V. Arrigler, H. Hägerstrand, Microtubes and nanotubes of a phospholipid bilayer membrane, *Journal of Physics A: Mathematical and General* 35 (2002) 1533–1549.
- [8] V. Kralj-Iglič, B. Babnik, D.R. Gauger, S. May, A. Iglič, Quadrupolar ordering of phospholipid molecules in narrow necks of phospholipid vesicles, *Journal of Statistical Physics* 125 (2006) 727–752.
- [9] Š. Perutková, M. Daniel, M. Rappolt, et al., Elastic deformations in hexagonal phases studied by small angle X-ray diffraction and simulations, *Physical Chemistry Chemical Physics* 13 (2011) 3100–3107.
- [10] V. Kralj-Iglič, A. Iglič, H. Hägerstrand, P. Peterlin, Stable tubular microexovesicles of the erythrocyte membrane induced by dimeric amphiphiles, *Physical Review E* 61 (2000) 4230–4234.
- [11] H. Jiang, G. Huber, R.A. Pelcovits, T.R. Powers, Vesicle shape, molecular tilt, and the suppression of necks, *Physical Review E* 76 (2007) 031908.
- [12] J.B. Fournier, Nontopological saddle-splay and curvature instabilities from anisotropic membrane inclusions, *Physical Review Letters* 76 (1996) 4436–4439.
- [13] V. Kralj-Iglič, S. Svetina, B. Žekš, Shapes of bilayer vesicles with membrane embedded molecules, *European Biophysics Journal* 24 (1996) 311–321.
- [14] V. Kralj-Iglič, V. Heinrich, S. Svetina, B. Žekš, Free energy of closed membrane with anisotropic inclusions, *European Physical Journal B* 10 (1999) 5–8.
- [15] A. Tian, T. Baumgart, Sorting of lipids and proteins in membrane curvature gradients, *Biophysical Journal* 96 (2009) 2676–2688.
- [16] T. Baumgart, B.R. Capraro, C. Zhu, S.L. Das, Thermodynamics and mechanics of membrane curvature generation and sensing by proteins and lipids, *Annual Review of Physical Chemistry* 62 (2011) 483–506.
- [17] D. Kabaso, N. Bobrovska, W. Gozdz, et al., On the role of membrane anisotropy and BAR proteins in the stability of tubular membrane structures, *Journal of Biomechanics* 45 (2012) 231–238.
- [18] F.C. MacKintosh, T.C. Lubensky, Orientational order, topology, and vesicle shapes, *Physical Review Letters* 67 (1991) 1169–1172.
- [19] N. Ramakrishnan, J.H. Ipsen, P.B.S. Kumar, Role of disclinations in determining the morphology of deformable fluid interfaces, *Soft Matter* 8 (2012) 3058–3061.
- [20] A. Iglič, B. Babnik, U. Gimsa, V. Kralj-Iglič, On the role of membrane anisotropy in the beading transition of undulated tubular membrane structures, *Journal of Physics A: Mathematical and General* 38 (2005) 8527–8536.
- [21] E. Chieriegatti, J. Meldolesi, Regulated exocytosis: new organelles for non-secretory purposes, *Nature Reviews. Molecular Cell Biology* 6 (2005) 181–187.
- [22] S.W. Hui, T.P. Stewart, L.T. Boni, P.L. Yeagle, Membrane fusion through point defects in bilayers, *Science* 212 (1981) 921–923.
- [23] L.V. Chernomordik, M.M. Kozlov, Mechanics of membrane fusion, *Nature Structural and Molecular Biology* 15 (2008) 675–683.
- [24] B. Ceccarelli, W. Hurlbut, A. Mauro, Turnover of transmitter and synaptic vesicles at the frog neuromuscular junction, *The Journal of Cell Biology* 57 (1973) 499–524.
- [25] J. Heuser, T. Reese, Evidence for recycling of synaptic vesicle membrane during transmitter release at the frog neuromuscular junction, *The Journal of Cell Biology* 57 (1973) 315–344.
- [26] M. Kozlov, V. Markin, Possible mechanism of membrane fusion, *Biofizika* 28 (1983) 242–247.
- [27] J. Urbanija, K. Bohinc, A. Bellen, et al., Attraction between negatively charged surfaces mediated by spherical counterions with quadrupolar charge distribution, *Journal of Chemical Physics* 129 (2008) 105101.
- [28] J. Zelko, A. Iglič, V. Kralj-Iglič, P.B.S. Kumar, Effects of counterion size on the attraction between similarly charged surfaces, *Journal of Chemical Physics* 133 (2010) 204901.
- [29] Y.W. Kim, J. Yi, P.A. Pincus, Attractions between like-charged surfaces with dumbbell-shaped counterions, *Physical Review Letters* 101 (2008) 208305.
- [30] R. Jahn, R. Scheller, SNAREs – engines for membrane fusion, *Nature Reviews. Molecular Cell Biology* 7 (2006) 631–643.
- [31] M. Jackson, E. Chapman, The fusion necks of Ca^{2+} -triggered exocytosis, *Nature Structural and Molecular Biology* 15 (2008) 684–689.
- [32] M. Stenovec, M. Kreft, I. Poberaj, W. Betz, R. Zorec, Slow spontaneous secretion from single large dense-core vesicles monitored in neuroendocrine cells, *FASEB Journal* 18 (2004) 1270–1272.
- [33] N. Vardjan, M. Stenovec, J. Jorgačevski, M. Kreft, R. Zorec, Subnanometer fusion necks in spontaneous exocytosis of peptidergic vesicles, *Journal of Neuroscience* 27 (2007) 4737–4746.
- [34] T. Fischer, Bending stiffness of lipid bilayers. III. Gaussian curvature, *Journal de Physique II* 2 (1992) 337–343.
- [35] M. Churchward, T. Rogasevskaia, D. Brandman, et al., Specific lipids supply critical negative spontaneous curvature – an essential component of native Ca^{2+} -triggered membrane fusion, *Biophysical Journal* 94 (2008) 3976–3986.
- [36] J. Israelachvili, *Intermolecular and Surface Forces*, Academic Press Limited, London, 1997.
- [37] R.D. Kamien, The geometry of soft materials: a primer, *Reviews of Modern Physics* 74 (2002) 953–971.
- [38] S. Kralj, R. Rosso, E.G. Virga, Curvature control of valence on nematic shells, *Soft Matter* 7 (2011) 670–683.
- [39] H. Poincaré, Sur les courbes tracées sur les surfaces algébriques, *Journal de Mathématiques Pures et Appliquées* 2 (1886) 151–217.
- [40] V. Vitelli, D.R. Nelson, Nematic textures in spherical shells, *Physical Review E* 74 (2006) 021711.
- [41] V. Vitelli, A.M. Turner, Anomalous coupling between topological defects and curvature, *Physical Review Letters* 93 (2004) 215301.
- [42] E.G. Virga, *Variational Theories for Liquid Crystals*, Chapman Hall, London, 1994.
- [43] R. Oda, I. Huc, M. Schmutz, S.J. Candau, F.C. MacKintosh, Tuning bilayer twist using chiral counterions, *Nature* 399 (1999) 566–569.